*Article*

# Detection of Targetable Genetic Abnormalities in Neuroblastoma Circulating Tumour DNA

Marina Danilenko [1,†], Sharanya Nath [1,2,3,†], Jack Baines [2], Freya Gordon [1,4], Swathi Merugu [1,5], Lisa M. Allinson [1], Aaron Potts [2], Bethany Collins [2], Angharad Goodman [2], Samuel E. Kidman [2], Ciaron McAnulty [2], David Jamieson [6] and Deborah A. Tweddle [1,7,*]

1 Wolfson Childhood Cancer Research Centre, Translational & Clinical Research Institute, Newcastle University Centre for Cancer, Herschel Building, Newcastle upon Tyne NE1 7RU, UK; marina.danilenko2@newcastle.ac.uk (M.D.); snath7@wisc.edu (S.N.); freya.gordon.24@ucl.ac.uk (F.G.); merugus@mskcc.org (S.M.); lisa.allinson@newcastle.ac.uk (L.M.A.)
2 Newcastle Genetics Lab., Newcastle upon Tyne Hospitals NHS Foundation Trust, Newcastle upon Tyne NE1 4EP, UK; jack.baines@nhs.net (J.B.); bethany.collins9@nhs.net (B.C.); sam.kidman@nhs.net (S.E.K.); ciaron.mcanulty@nhs.net (C.M.)
3 Division of Hematology, Medical Oncology and Palliative Care, Department of Medicine, School of Medicine and Public Health, University of Wisconsin, Madison, WI 53726, USA
4 Childhood Brain Tumour Research Group, Developmental Biology and Cancer, Great Ormond Street Institute of Child Health, University College London, London WC1N 1EH, UK
5 The Immune Monitoring Facility, Ludwig Centre for Cancer Immunotherapy, Memorial Sloan Kettering Cancer Center, New York, NY 10021, USA
6 Translational & Clinical Research Institute, Newcastle University Centre for Cancer, Paul O'Gorman Building, Newcastle upon Tyne NE2 4HH, UK; david.jamieson@newcastle.ac.uk
7 Department of Paediatric Oncology, Great North Children's Hospital, Newcastle NE1 4LP, UK
* Correspondence: deborah.tweddle@newcastle.ac.uk
† These authors contributed equally to this manuscript and are to be considered joint first authors.

## Abstract

Neuroblastoma (NB) is an aggressive childhood cancer requiring intensive multimodal therapies in high-risk (HRNB) patients. Currently, invasive surgical biopsies are required to classify NB risk group and assign treatment based on the tumour genetic profile. Circulating tumour DNA (ctDNA) obtained from blood samples can be used to identify tumour biomarkers. Here we applied targeted next-generation sequencing (tNGS) using a panel of 42 genes to analyse 32 NB ctDNA samples for the presence of single-nucleotide variants and copy number changes from 28 patients in all NB risk groups. In two additional ctDNA samples, droplet digital PCR was used to detect hotspot *ALK* variants. Pathogenic mutations with a variant allele frequency (VAF) > 1% were identified in 13/32 (41%) ctDNA samples. *ALK* and *PTPN11* were the most frequent, each being detected in 4/32 (13%) samples, together with oncogene amplifications. Targeted NGS of ctDNA detected actionable variants, including those absent in the diagnostic primary tumour due to spatial and temporal heterogeneity. Our findings confirm the usefulness of ctDNA in detecting genetic abnormalities in NB.

Keywords: circulating tumour DNA; liquid biopsy; next-generation sequencing; ddPCR; paediatric cancer; neuroblastoma

## 1. Introduction

Neuroblastoma (NB) is the most frequent extracranial solid malignancy in children below the age of 5 years [1]. Around 100 new cases of NB are diagnosed in the UK each

year, and about half of these are high-risk neuroblastoma (HRNB) with a 5-year event-free survival (EFS) below 50%.

Diagnosis and risk group assignment for NB requires an invasive tumour biopsy, which may be associated with considerable morbidity, particularly in patients below the age of 18 months [2]. An alternative non-invasive means of performing genetic studies in patients with solid tumours is through liquid biopsy sampling to assess circulating tumour cells and circulating tumour DNA (ctDNA) [3,4]. Liquid biopsies are not only safer in young patients but also provide knowledge of intra-tumoural heterogeneity [4].

Cell-free DNA (cfDNA) includes circulating short fragments of double-stranded DNA found in peripheral blood. Circulating tumour DNA (ctDNA) is the fraction of cfDNA originating from tumour tissue in cancer patients and generally constitutes less than 0.1–10% of the total cfDNA present in peripheral blood [5]. Recent studies of NB [6–8] and other cancers [9,10] have established that genome-wide DNA sequencing from blood plasma is a promising method for assessing tumour burden. These studies demonstrate, that in metastatic cancer, ctDNA in plasma reflects a composite genetic profile of all existing tumours in a patient. The half-life of ctDNA ranges from 16 to 150 min [10] and helps to record real time intra-tumoural events.

ctDNA analyses offer the potential to characterise NB tumour biology, which is not possible by studying the primary tumour alone. The purpose of this study was to detect and characterise the genetic abnormalities in NB ctDNA collected from patients across different risk groups using targeted next-generation sequencing (tNGS), and in a subset droplet digital PCR (ddPCR), and to compare the findings with matched primary tumour data where available.

## 2. Results

### 2.1. Pathogenic Variants Identified Following ctDNA Variant Filtering

On average, the pipeline called $n$ = 120 raw variants per sample. After stringent filtering (see Section 4), 12/32 ctDNA samples had 15 driver variants in total (Table 1). Among these, five were pathogenic *ALK* variants, three were pathogenic *TP53* variants and four pathogenic *PTPN11* variants (Table 1). In total, 10/15 identified ctDNA variants were predicted by in silico tools to have a detrimental impact on protein function and were recorded in the COSMIC database (Table 1) [11]. The remaining variants were classified either as 'likely pathogenic' or 'variants of uncertain significance' (VUSs), as all of them had low 'rare exome variant ensemble learner' (REVEL) [12] scores (≤0.7) and were not reported in the literature and/or had no COSMIC presence. Finally, two out of three germline DNA samples and two out of four cell-line control DNA samples had driver variants. Previously reported findings were confirmed in the cell lines (Table 1).

**Table 1.** Pathogenic variants detected in ctDNA (ctD), germline DNA (gD) and cell-line DNA samples. All variants were identified as missense variants, apart from *NF1*, which was identified as a splice donor. Abbreviations: Del—deleterious, POD—possibly damaging, PRD—probably damaging, B—benign, Chr—chromosomal. REVEL score > 0.7 = pathogenic. 1 = SHSY5Y cell line, 2 = SKNBE(2c) cell line. [a,b] = Identifies ctDNA and matched gDNA pairs. [c] = Identifies paired samples from the same patient at diagnosis and relapse.

| Sample | VAF | Variant Gene | Chr. Location | Base Change | Protein Change | COSMIC ID | SIFT Score | Polyphen Score | REVEL Score |
|---|---|---|---|---|---|---|---|---|---|
| ctD4 | 2.85 | *ALK* | chr2 (p23.2) | c.(3824G>A) | p.(R1275Q) | COSV66555567 | Del (0) | PRD (1) | 0.885 |
| ctD4 | 28.5 | *ALK* | chr2 (p23.2) | c.(3522C>A) | p.(F1174L) | COSV66556325 | Del (0.03) | POD (0.641) | 0.752 |

**Table 1.** *Cont.*

| Sample | VAF | Variant Gene | Chr. Location | Base Change | Protein Change | COSMIC ID | SIFT Score | Polyphen Score | REVEL Score |
|---|---|---|---|---|---|---|---|---|---|
| ctD10 | 1.38 | *ALK* | chr2 (p23.2) | c.(3509T>A) | p.(I1170N) | COSV66589132 | Del (0) | PRD (1) | 0.906 |
| ctD10 | 26.16 | *KRAS* | chr12 (p12.1) | c.(35G>T) | p.(G12V) | COSV55497419 | Del (0) | PRD (0.972) | 0.91 |
| ctD10 | 3.61 | *PTPN11* | chr12 (q24.13) | c.(179G>C) | p.(G60A) | COSV61006397 | Del (0.01) | PRD (0.953) | 0.907 |
| [a] ctD11 | 84.88 | *TP53* | chr17 (p13.1) | c.(537T>A) | p.(H179G) | COSV52673406 | Del (0) | PRD (0.98) | 0.79 |
| [a] gD1 | 1.4 | *TP53* | chr17 (p13.1) | c.(537T>A) | p.(H179Q) | COSV52669519 | Del (0) | PRD (0.98) | 0.79 |
| ctD13 | 3.33 | *ALK* | chr2 (p23.2) | c.(3522C>A) | p.(F1174L) | COSV66556325 | Del (0.03) | POD (0.641) | 0.752 |
| [b] ctD15 | 35.8 | *PTPN11* | chr12 (q24.13) | c.(922A>G) | p.(N308D) | COSV61006575 | Del (0.03) | B (0.134) | 0.838 |
| [b] gD2 | 43.9 | *PTPN11* | chr12 (q24.13) | c.(922A>G) | p.(N308D) | COSV61006575 | Del (0.03) | B (0.134) | 0.838 |
| ctD16 | 4.34 | *PTPN11* | chr12 (q24.13) | c.(181G>T) | p.(D61Y) | COSV61004841 | Del (0) | PRD (0.997) | 0.933 |
| ctD17 | 2.26 | *NRAS* | chr1 (p13.2) | c.(181C>A) | p.(Q61K) | COSV54736310 | Del (0.01) | POD (0.709) | N/A |
| [c] ctD20 | 91.64 | *TP53* | chr17 (p13.1) | c.(840A>T) | p.(R280S) | COSV52782181 | Del (0.03) | POD (0.843) | 0.878 |
| [c] ctD21 | 83.4 | *TP53* | chr17 (p13.1) | c.(840A>T) | p.(R280S) | COSV52801834 | Del (0.03) | POD (0.843) | 0.878 |
| ctD22 | 29.03 | *ALK* | chr2 (p23.2) | c.(3824G>A) | p.(R1275Q) | COSV66555567 | Del (0) | PRD (1) | 0.885 |
| ctD25 | 18.7 | *PTPN11* | chr12 (q24.13) | c.(226G>C) | p.(E76Q) | COSV61004751 | Del (0.01) | PRD (0.979) | 0.733 |
| ctD28 | 2.2 | *CREBBP* | chr16 (p13.3) | c.(4478T>A) | p.(I1493K) | COSV52129182 | Del (0) | PRD (0.991) | 0.929 |
| 1 | 44.4 | *KRAS* | chr12 (p12.1) | c.(35G>T) | p.(G12V) | COSV55497419 | Del (0) | PRD (0.972) | 0.91 |
| 1 | 50.9 | *SMARCA4* | chr19 (p13.2) | c.(2917C>T) | p.(R973W) | COSV60787034 | Del (0) | PRD (1) | 0.86 |
| 1 | 49.6 | *ALK* | chr2 (p23.2) | c.(3522C>A) | p.(F1174L) | COSV66555460 | Del (0.03) | POD (0.641) | 0.752 |
| 2 | 99.1 | *TP53* | chr17 (p13.1) | c.(404G>T) | p.(C135F) | COSV52680475 | Del (0) | PRD (1) | 0.96 |
| 2 | 100 | *NF1* | chr17 (q11.2) | c.(1989_2001del) | p.(G663fs) | N/A | N/A | N/A | N/A |

### 2.2. A High Proportion of Variants Were Identified in NB ctDNA but Not in NB Tumours

Twenty-two ctDNA samples had matching tumour NGS data available, and thus 16 variants could be compared between liquid biopsies and NB tumours (Figure 1). Strikingly, only nine variants were identified in both ctDNA and matching tumours. The other seven variants were either present in ctDNA only (five mutations: two in *ALK*, one in *PTPN11*, one in *NRAS* and one in *CREBBP*) or only identified in the NB tumours (one mutation in *ATM* and one in *CHK2*) (Figure 1).

### 2.3. Spatial and Temporal Heterogeneity of Heterozygous ALK Mutations

*ALK* was found to be the most commonly mutated gene in this study. A total of five driver *ALK* variants were observed in four ctDNA samples (Figure 1). Three hotspot kinase domain mutations (R1275Q, F1174L and I1170N) were observed (Figure 2A). R1275Q was present in two ctDNA samples (ctD4 and ctD22), and F1174L was present in two ctDNA samples (ctD4 and ctD13). I1170N was present in one ctDNA sample (ctD10) (Table 1).

The most striking observation to emerge from the *ALK* variant data was from sample ctD4. The Venn diagram (Figure 2B) shows that two variants, encoding R1275Q and F1174L, were detected in the plasma sample from diagnosis, with VAFs of 2.85% and 28.5%, respectively. However, in the diagnostic primary tumour only the R1275Q variant was

detected by Sanger sequencing and Agena Mass Array [13] (VAF: 32.0%) (Figure 2B). In a separate plasma sample analysed by ddPCR at the end of treatment, neither R1275Q nor F1174 variants were detected. Figure 2C shows ddPCR results for F1174L at the end of treatment and relapse; results for R1275Q are not included. In a metastatic relapse sample and a plasma relapse sample, 3 months later only the F1174L mutation was detected by targeted NGS from SMPaeds data on the metastatic tumour [14,15] (VAF: 46.1%) and by digital-droplet PCR (ddPCR) (VAF: 98%) on the plasma (Figure 2B,C). R1275Q was not detected in either tumour or plasma at relapse. This patient did not receive an ALK inhibitor at any stage of treatment. This data reflects the presence of spatial and temporal intra-tumoural heterogeneity. It also shows that ctDNA is more representative of malignant clones promoting NB relapse than the primary tumour.
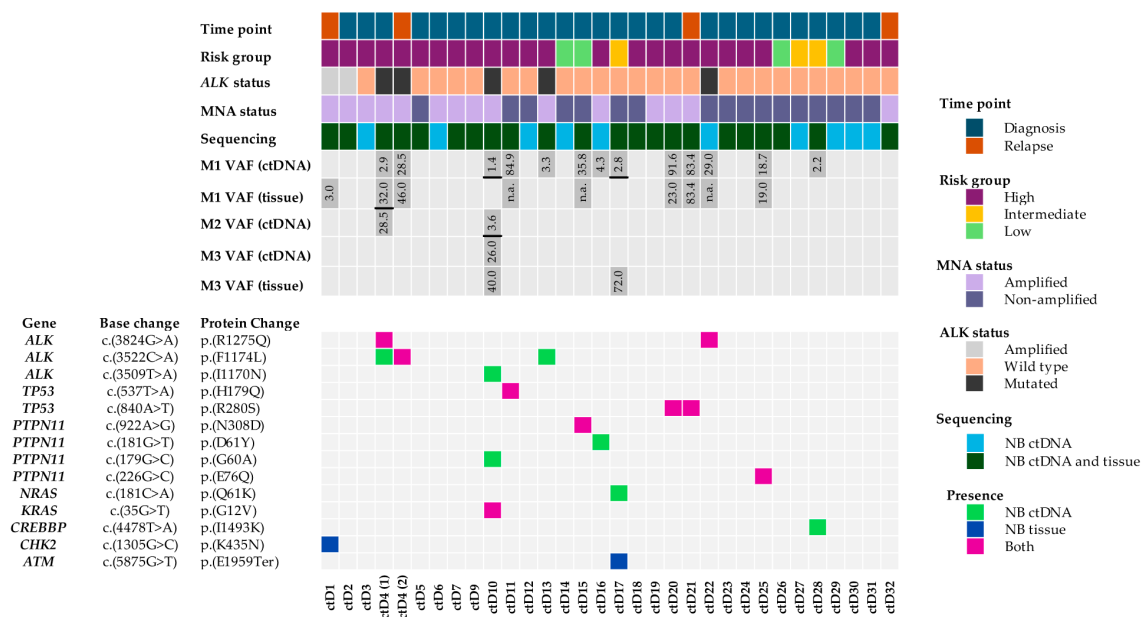


**Figure 1.** Oncoplot showing comparison of sequencing data between matched NB ctDNA and NB tumours. ctDNA (1–32) is displayed on the *x*-axes. ctD8 was excluded from further analysis, as the cfDNA concentration was below the threshold value of 20%. Information about patient cohort, VAFs (variant allelic frequencies) and the identified variants are displayed on the *y*-axes. Three samples had more than one mutation, and hence there are VAFs for M1, M2 and M3 displayed (with M1 being the top one, M2 the middle one and M3 the bottom one on the oncoplot). VAFs from different variants are separated by black lines. ctD4 is included twice, as an additional relapse sample was obtained from this patient and assessed by ddPCR. Samples 20 and 21 are paired diagnosis and relapse samples from the same patient.

### 2.4. Pathogenic, Homozygous Somatic TP53 Mutations

In this study four *TP53* pathogenic variants with high VAFs were observed in the DNA binding domain of the *TP53* gene (Table 1 and Figure 3A). Three were found in ctDNA and one in a germline DNA sample (Table 1). Observed protein changes were as follows: H179Q in ctD11 and gD1 and R280S in ctD20 and ctD21. Figure 3B shows a homozygous *TP53* variant detected in the diagnosis plasma sample (ctD20), post-chemotherapy primary tumour and relapse plasma (ctD21) samples. The lower VAF for the post-chemotherapy tumour reflects the lower tumour cell content (estimated: 30%, calculated: 19%). Homozygosity was confirmed by 17p loss of heterozygosity (Table A1). In another diagnostic case (ctD11), with a homozygous somatic *TP53* mutation (VAF: 84.9%) caused by concomitant 17p loss (Table A1), the matching diagnostic germline sample had a VAF of 1.4%, suggesting that the gDNA was contaminated with tumour DNA when collected (Table 1).
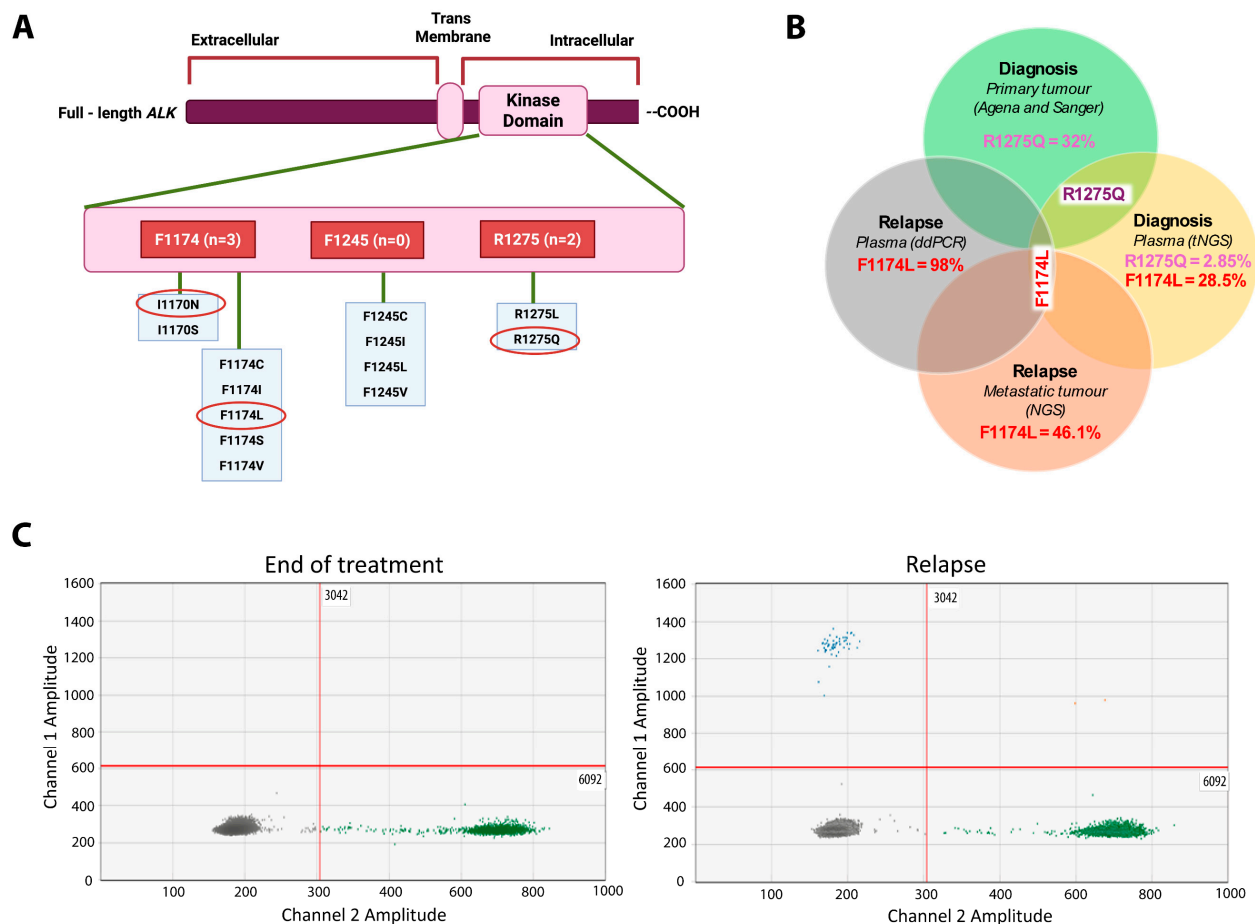
**Figure 2.** Spatial and temporal heterogeneity of *ALK* variants. (**A**) Distribution of pathogenic *ALK* positions across the tyrosine kinase (TKD) domain within ctDNA. Numbers in red rectangles reflect three cases identified with *ALK* F1174 mutations, no cases with an *ALK* F1245 mutation and two cases with an *ALK* R1275 mutation. (**B**) Venn diagram showing the spatial and temporal heterogeneity of activating *ALK* variants in the tumour and plasma obtained from patient ctD4. (**C**) *ALK* ddPCR on ctDNA samples collected at the end of treatment when the patient was in remission and 3 months later at relapse. Grey droplets are those with no DNA attached, while green droplets represent the wild-type *ALK* allele. F1174L variant (visualised as blue droplets) was not detected at the end of treatment but was identified at relapse.

## 2.5. Heterozygous, Pathogenic PTPN11 Variants

Pathogenic *PTPN11* variants (RAS-MAPK pathway gene family) were observed in five samples (Table 1). A pathogenic germline variant, *PTPN11* N308D, in both ctD15 and gD2 (germline DNA) was identified in a patient with Noonan syndrome and low-risk NB [16–18] with VAFs of 35.8% and 43.9%. In the other three cases, activating *PTPN11* mutations were detected within the N terminal domain: G60A (VAF: 3.6%) in the case with a concomitant *KRAS* and *ALK* mutation (ctD10) and in the other two cases at the known hotspots E76Q (VAF: 18%) and D61Y (VAF: 4.34%).

## 2.6. Oncogene Amplifications Detected in ctDNA

Higher values for coverage were observed in regions corresponding to known oncogene amplification sites (compared to other genes) (Figure 4).

*MYCN* amplification was detected in 14/32 ctDNA samples and confirmed in 2 known *MYCN* amplified cell lines (Figures 4 and 5A,B). This was consistent with the amplification status detected by Illumina CytoSNP-850k arrays (Table A1). Furthermore, co-amplification of *ALK* and *MYCN* was observed in the ctDNA samples ctD1 and ctD2, taken from the same

patient at diagnosis and relapse, and was consistent with SNP array results in the primary tumour and ctDNA [19] (Figure 5C). *CDK4* amplification, previously associated with a poor prognosis in NB patients [20,21], was detected in ctD3 and confirmed in the NB-1691 cell line (Figure 5A,D). The presence of *MDM2* amplification was also confirmed in the NB-1691 cell line (Figure 5A) and the presence of *CCND1* amplification in ctD3 (Figure 5D). However, neither *ALK* amplification in NB-1691 cells [22] nor *FGFR1* amplification in ctD19, which were evident on SNP arrays (Table A1), were detected in ctDNA (Figures 4 and 5).
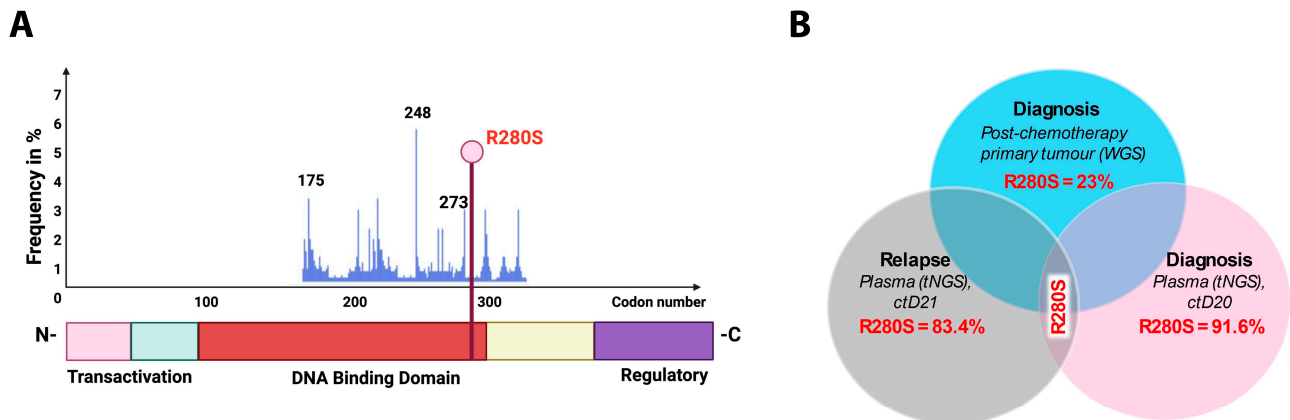


**Figure 3.** Longitudinal analysis of a homozygous *TP53* variant detected in NB ctDNA and the primary tumour from the same patient. (**A**) Position of the *TP53* variant within the DNA binding domain. (**B**) Venn diagram depicting the *TP53* variant detected across three samples: the diagnostic plasma sample, the post-chemotherapy resected primary tumour and the relapse plasma sample. WGS—whole-genome sequencing.
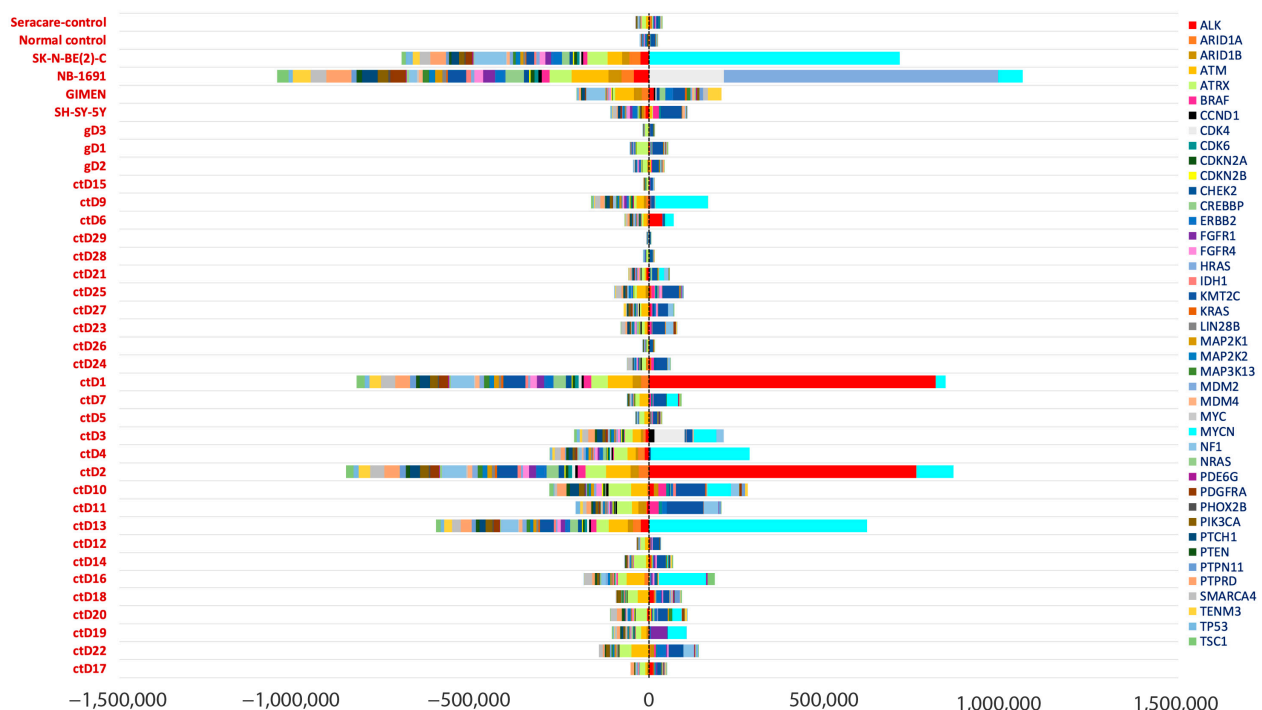


**Figure 4.** Copy number aberrations detected in NB ctDNA. Bar graph shows inverse z-scores for each target region amplified compared to all other regions in the same sample. The regions with a significant copy number change (amplification or gain) are highlighted with longer bins in the positive quadrant. Numerical coverage data could not be retrieved for ctD30, ctD31 and ctD32, so these samples were omitted. ctD1 and ctD2 and ctD20 and 21 are paired samples at diagnosis and relapse, respectively.
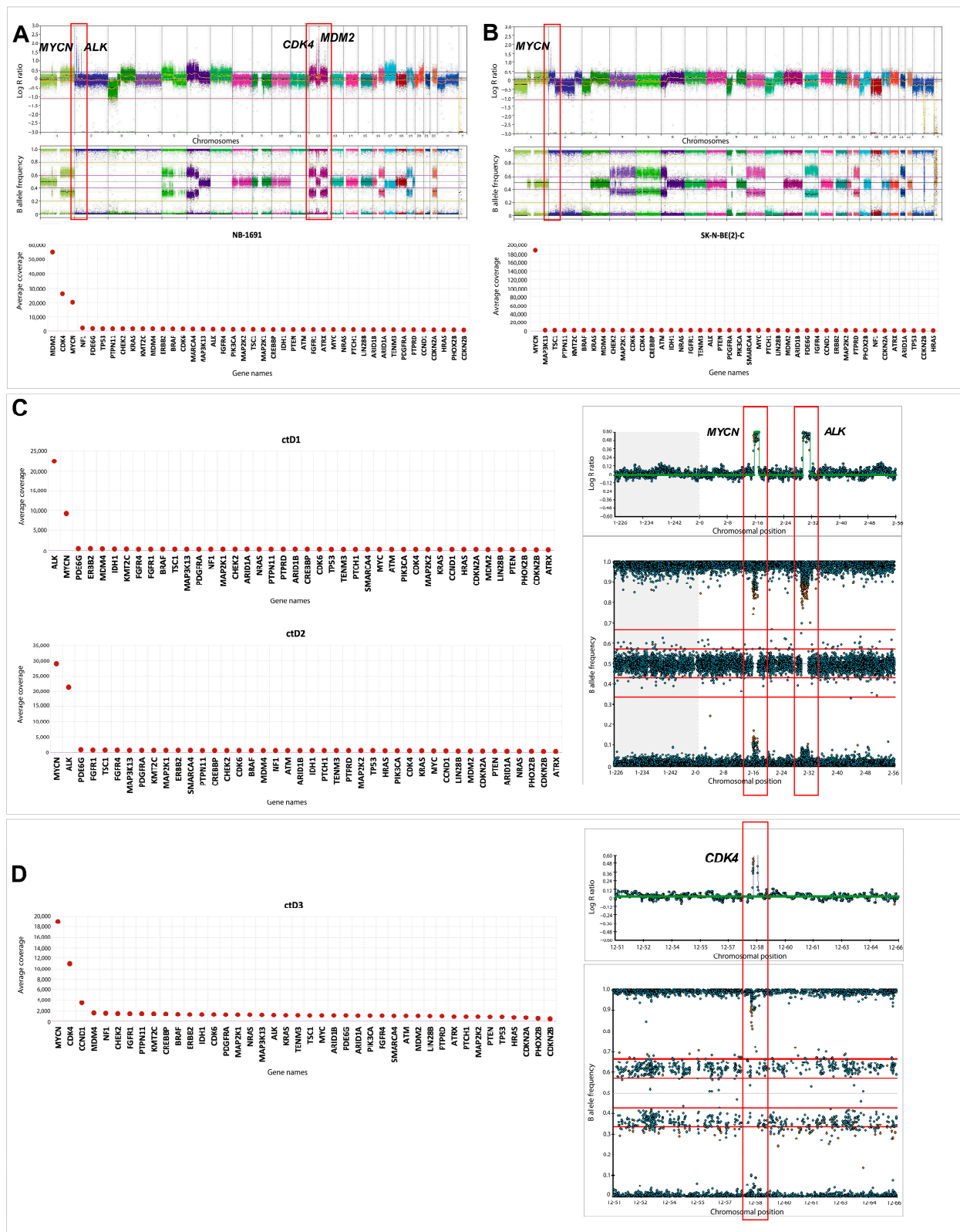
**Figure 5.** Amplification of *MYCN* (MNA), *ALK* and *MDM2* oncogenes. The 2D line graph depicts the relative coverage of all 42 targeted genes compared to the respective SNP array data from primary tumours or ctDNA. (**A**) NB-1691 cell line: *MYCN*, *CDK4* and *MDM2* amplification, but not *ALK*, were detected by relative coverage analyses compared with the SNP array. (**B**) MNA in SK-N-BE(2)-C cell line. (**C**) *ALK* amplification and MNA detected in ctD1 and ctD2 paired samples. (**D**) MNA, *CDK4* and *CCND1* amplification in ctD3.

## 3. Discussion

The use of liquid biopsy in the management of patients with cancer, either along-side traditional histopathology or as the primary method of obtaining clinically relevant biomarker data, affords clinicians access to real-time tumour monitoring and the ability to detect druggable targets as a tumour evolves. NB frequently metastasises to bone and bone marrow, making liquid biopsy particularly useful for patients with metastatic NB. CfDNA can be extracted from as little as 0.5–2 mL of plasma [23–25] and is a viable alternative to invasive biopsies, which increase morbidity in young patients.

Using a targeted gene panel and sequencing ctDNA from plasma samples, we aimed to detect driver events and oncogenic amplifications in ctDNA and to compare these with tumour biopsy samples, where available. Results from this study showed that the bioinformatics pipeline was able to detect all clinically relevant variants, including those with low VAFs (>1%), in ctDNA. Strikingly, 7/16 identified driver ctDNA variants for which tumour NGS data was available, were only present in ctDNA and not in NB tissue. This can be explained by the intra-tumoural heterogeneity of NB when the variants were absent in the biopsied tumour regions while present in ctDNA representing a pool of variants from multiple tumour regions [15,26]. All the variants detected only in ctDNA were at a VAF of <5% and thus likely to be sub-clonal or due to low ctDNA content in the blood. A threshold of 5% has been assigned for most clinical NGS reporting on the bulk tumour, and thus variants with a VAF < 5% could be omitted during data analyses. In two cases, DNA from the NB tumour contained *CHK2* (VAF = 3%) and *ATM* (VAF = 72%) mutations, which were absent in paired ctDNA at the same time point. This could be due to low ctDNA shedding into the blood or variants being sub-clonal. Tumour-only mutations have been previously reported in paired tumour and ctDNA studies and are typically explained by low levels of ctDNA in the patient's blood [15,26].

Importantly, an *ALK* variant (F1174L) not detected in the diagnostic primary tumour biopsy using the Agena Mass Spectrometer assay, which detects mutations at a VAF of 1.3% [13], was present in diagnostic ctDNA (ctD4), the metastatic relapse biopsy and relapse ctDNA (Figure 2B). This confirms that ctDNA is more reflective of the global genomic variation in a tumour as it overcomes the problem of intra-tumoural heterogeneity missed by a single-site biopsy. In ctD4 two *ALK* mutations were identified in diagnostic ctDNA (R1275Q and F1174L), in line with other ctDNA studies reporting several *ALK* mutations in a single ctDNA sample [15,26–29]. This case demonstrates both spatial and temporal heterogeneity with different *ALK* mutations detected in the diagnostic primary tumour (R1275Q) and relapsed metastatic tumour (F1174L), as well clonal evolution with loss of the R1275Q mutation between diagnostic and relapse ctDNA, together with an increase in the VAF of the F1174L mutation. The clonal evolution occurred in the absence of selective pressure from patient treatment with an ALK inhibitor.

In keeping with other studies [30,31], pathogenic *ALK* mutations were the commonest mutations in this study, while *PTPN11* mutations were the second most frequent (Table 1 and Figure 1). A study by Ackermann et al. [32] sequenced NB genomes, where they also found *PTPN11* to be commonly mutated. This highlights the importance of developing treatments for *PTPN11* mutated NB, the efficacy of which could be tracked by serial ctDNA monitoring. The Ackermann study reported ALK-RAS pathway mutations to be associated with poor outcomes in all NB risk groups when associated with telomere maintenance mechanisms. In our study, ctD10 harboured two RAS-MAPK (*KRAS*-G12V and *PTPN11*-G60A) mutations and an *ALK*-I1170L mutation, in addition to *MYCN* amplification (a telomere maintenance mechanism) (Table 1). We also detected four ctDNA samples (ctD10, ctD16, ctD20 and ctD21) having RAS-MAPK pathway or *TP53* mutations alongside *MYCN* amplification and hence falling into a very poor prognostic group.

The bioinformatic pipeline was able to detect *MYCN*, *ALK*, *CDK4* and *MDM2* amplifications. However, *ALK* amplification in NB-1691 cells [22] and *FGFR1* amplification in ctD19 were not detected, most likely due to only partial amplification of these oncogenes in regions not covered by the gene panel. Furthermore, the tNGS approach failed to detect other copy number events, as the gene panel was limited to 42 known target genes and did not cover the entire genome (Table A2). Whole-exome sequencing (WES) or low-coverage WGS would be required to detect all copy number changes in these samples

Liquid biopsy-based analysis of ctDNA offers several advantages in the management of NB. Firstly, it is a non-invasive procedure that can be performed longitudinally, allowing for monitoring of disease progression and treatment response over time, as well as early relapse detection. Secondly, it provides a comprehensive assessment of tumour heterogeneity, enabling detection of genetic alterations that may not be captured by single-site tumour biopsies. Thirdly, liquid biopsy can identify actionable variants, guiding personalised treatment decisions.

While our study highlights the potential of ctDNA monitoring in NB, it is limited by its size and the use of mainly diagnostic samples with longitudinal samples in only three cases. The longitudinal testing of plasma samples provides more information about NB progression over time, uncovering possible mechanisms of treatment resistance and relapse, as recently reported by studies of *ALK* mutation tracking in ctDNA collected from NB patients treated with *ALK* inhibitors [26,28,29]. Previous studies reported both reductions in the VAFs of *ALK* mutations in longitudinal ctDNA sampling during successful patient treatment with ALK inhibitors [7,15,26,28,29,33,34] but also the emergence of resistance mutations, including both bypass mutations, particularly of the RAS-MAPK pathway [26,28,29,34], as well as compound *ALK* mutations [29]. Importantly, one study also reported loss of *ALK* mutations in some patients who relapsed during treatment with the third-generation ALK inhibitor lorlatinib, due to selection for *ALK* wild-type clones by lorlatinib treatment [29]. Furthermore, we have previously reported selection for *ALK* wild-type clones in tumour DNA from two patients between diagnosis and relapse in the absence of ALK inhibitor treatment [13]. These studies emphasise the importance of serial ctDNA monitoring for *ALK* mutations in patients with NB, particularly when treating patients with ALK inhibitors.

In conclusion, our study confirms the potential of liquid biopsy, specifically ctDNA analysis, to study NB in a non-invasive way.

## 4. Materials and Methods

### 4.1. Plasma and Cell-Line Samples

Plasma and germline DNA samples were obtained from VIVO biobank (formerly the Children's Cancer and Leukaemia Group (CCLG) Tissue Bank) (study number 2021 BS 03). The NGS study included *n* = 41 samples, of which *n* = 32 were ctDNA samples from NB patient plasma, including *n* = 3 paired samples (2 paired diagnosis and relapse and 1 paired blood and bone marrow plasma), *n* = 3 germline DNA, *n* = 4 control NB cell-line DNA (SH-SY-5Y, NB-1691, SK-N-BE(2)-C and GIMEN) and *n* = 2 control samples, one a synthetic control (Seraseq ctDNA. Complete AF0.1%, Seracare) (Seracare, Milford, MA, USA) and the other a normal genomic DNA control (Table A1). Two additional plasma samples (from the end of treatment and three months later at relapse) from the ctD4 patient were obtained and used for ddPCR. In total, 28 NB cases were studied: 4 low risk, 3 intermediate risk and 21 high risk (Figure 1 and Table A1).

### 4.2. DNA Extraction

DNA from 4 cell lines and ctDNA from 0.5 mL plasma were extracted using EZ1 Advanced XL (QIAGEN, Hilden, Germany) kits: the EZ1 DNA 200 µL Blood Kit for plasma samples and the EZ1 DNA Tissue Kit for cell-line pellets, according to the manufacturer's instructions. cfDNA content was assessed using the Agilent TapeStation 4200 (Agilent, Santa Clara, CA, USA with the cell-free DNA ScreenTape assay. Sample ctD8 was excluded from further analysis, as the cfDNA concentration was only 6%, below the threshold value of 20%. The library preparation method also incorporated unique molecular indices (UMIs) ligated to the ends of DNA fragments. The UMI code is a sequence of short nucleotides that uniquely identifies each molecule in a sample library, enabling greater precision during sequencing and error correction. The prepared libraries were quality assessed using Bioanalyzer 2400 High Sensitivity D1000 chip assays (Agilent, Santa Clara, CA, USA) by quantifying fragments between 35 and 1000 bp. The size interval used for library preparation was approximately between 200 and 400 bp, where the cfDNA fragment peak formed. The prepared libraries were also quantified using the Qubit Fluorometer 2.0—double-stranded DNA high-sensitivity assay (ThermoFisher, Waltham, MA, USA).

### 4.3. Library Preparation and Next-Generation Sequencing

Sequencing library preparation for ctDNA samples was performed according to the manufacturer's instructions using a QIAseq Targeted Custom DNA Panel of 42 genes (Table A2). The gene panel was compiled according to recommendations of the SIOPEN Biology Group [35]. Targeted NGS (Illumina NextSeq 550 System (Illumina, Inc., San Diego, CA, USA)) was performed on *n* = 31 patient cfDNA samples, *n* = 4 cell-line DNA samples, *n* = 3 germline DNA samples and *n* = 2 control DNA samples. Raw reads from the NextSeq550 were aligned and variant calling was performed using CLC Genomics Workbench 22 (CLC Bio, version 22.0, Aarhus, Denmark). An analysis of the UMI coverage per gene was carried out across all samples.

### 4.4. Variant Filtering

The mean read depth was calculated to be 2228x after excluding the read depth of over- and underrepresented amplified genes and genes on the X chromosome, consistent with the manufacturers' specifications of a mean read depth of 2500x for 20 samples on a mid-output flow cell with the QiaSeq kit (QIAGEN). Variants with coverage < 100× and frequencies < 0.5% were filtered out. CLC Genomics workbench tools software was used to remove sequencing artefacts, PCR duplicates and recurrent variants. The resulting variants were then annotated using the Ensembl Variant Effect Predictor (VEP) [36] with Genome Aggregation Database (gnomAD r2.1, exomes only [37]) population frequencies, 'Sorting Intolerant from Tolerant' (SIFT 5.2.2) [38] algorithm scores, 'Polymorphism Phenotyping v2' (PolyPhen 2.2.2) [39] scores (range from 0 to 1; 0 = most likely benign, 1 = most likely damaging), 'rare exome variant ensemble learner' (REVEL) [12] scores (range from 0 to 1; 0 = likely benign, 1 = likely pathogenic) and COSMIC IDs [11]. Using a standard approach, the pipeline filtered out germline variants by removing the SNPs found in the 'dbSNP common' database [40] (dbSNP build 151, with ≥1% minor allele frequency (MAF) present in any of the five super-populations). Further stringent filtering for germline variants was performed manually by annotating the variants with gnomAD frequencies using VEP, excluding variants occurring in different population groups (gnomAD r2.1, exomes-only database) with a frequency of more than 1.0%. Furthermore, germline data was used from WGS from blood samples corresponding to ctD19, ctD20, ctD23, ctD25, ctD26 and ctD28 sequenced at 30x coverage (NHS England Whole Genome Sequencing (WGS) service). In

these cases, the final filtered variants generated were subjected to a comparative analysis against the germline variants identified in their matched WGS data.

### 4.5. Coverage Analysis

An analysis of the UMI coverage per gene was carried out across all samples and graphs were plotted. The UMI coverage was assessed using two metrices, relative UMI coverage (average coverage) and UMI read depth, which helped evaluate the reliability of the tNGS panel in covering all the targeted regions. To validate the coverage data to correctly detect gene amplification status, the results, wherever possible, were compared with SNP array data generated from Illumina CytoSNP-850k arrays using Illumina BlueFuse multi v4.4 software or Nexus Copy Number v10.0 software (Bionano Genomics Inc., San Diego, CA, USA).

### 4.6. Classification of Somatic Variants

Classification of filtered variants was determined by considering both the biological and clinical relevance of the data [5]. The potential pathogenicity of variants was determined using SIFT [38], PolyPhen-2 [39], REVEL [12] scores and COSMIC [11] presence. Variants not classified previously in COSMIC or from a literature review were not discarded but retained for further investigation. The list of somatic driver variants was also compared with those obtained from analysis of the primary or metastatic tumours using WGS ($n = 9$) or a different targeted or whole-exome sequencing platform ($n = 13$). This included NGS from Stratified Medicine Paediatrics (SMPaeds) testing [14] or tNGS using a SIOPEN 38 gene panel [35] where available, together with results of *ALK* sequencing using Sanger sequencing or Agena Mass Spectrometer arrays [13] (Figure 1).

### 4.7. ddPCR

High-sensitivity testing for the ALK c.3522C>A p.(F1174L) and c3824G>A p.(R1275Q) variants was performed by droplet digital PCR (ddPCR) using commercially designed primers and probes obtained from Bio-Rad (assay ID numbers: dHsaMDV2516768 ALKp.R1275Q and dHsaMDV2010083ALK p.F1174L c.3522C>A). Cell-free DNA extracted from peripheral blood was amplified by standard PCR methods and fragmented by restriction digest using HaeIII. PCR products were then separated using the Bio-Rad QX-200 ddPCR system following standard Bio-Rad protocols. Analysis was performed using QX Manager Software Standard Edition v2.1 obtained from BioRad (Hercules, CA, USA). The sequence for the *ALK* F1174L c.3522C>A primer is hg19 | chr2:29443634-29443756, and for the *ALK* p.R1275Q primer the sequence is hg19 | chr2:29432603-29432725.

### 4.8. Statistical Analyses

Target-region coverage analysis was carried out for all samples using the CLC Genomics Workbench tools. The resulting numerical data per targeted region per gene was used to calculate a z-score for the determination of CNVs from coverage data [41].

$$Z = \frac{x - \mu}{\sigma}$$

where x = raw score, $\mu$ = mean of data array and $\sigma$ = standard deviation of the data array.

**Author Contributions:** Conceptualisation, D.A.T., C.M. and M.D.; methodology, S.N. and J.B.; software, S.E.K., S.N. and J.B.; validation, L.M.A., A.G. and A.P.; formal analysis, S.N., J.B., M.D. and B.C.; investigation, S.N., M.D., J.B. and B.C.; resources, S.M. and D.J.; data curation, D.A.T., S.N. and J.B.; writing—original draft preparation, M.D. and S.N.; writing—review and editing, D.A.T., M.D. and F.G.; visualisation, M.D., S.N. and J.B.; supervision, D.A.T. and C.M.; project administration, J.B.

# Appendix A

*Appendix A.1*

**Table A1.** Samples used in the ctDNA study with existing SNP array data from the primary tumour. ctD8 was excluded from further analysis, as the cfDNA concentration was below the threshold value of 20%. [a,b,c] = paired ctDNA samples; [a,b] were obtained from the same patient at diagnosis and relapse and [c] was obtained from ctDNA from the same patient from blood and bone marrow at diagnosis. [d,e,f] = ctDNA and matched gDNA pairs. Abbreviations and symbols: NB—Neuroblastoma; Int—Intermediate risk; Int ** = localised, non-MNA, >18 months of age, unfavourable histology; PB—Peripheral blood; BM—Bone marrow; R—Relapse; D—Diagnosis; * denotes cases where SNP array performed on ctDNA [19]; CN-LOH = copy neutral loss of heterozygosity; MNA—*MYCN* amplified; non-MNA—Non-*MYCN* amplified.

| Sample Name | Sample Type | NB Risk Group and *MYCN* Status | Time Point | SNP Array Data Gain | Loss |
|---|---|---|---|---|---|
| [a] ctD1 | Plasma (PB) | High MNA | R | * 1q, 17q, 18q. *ALK* amplification | * 1p, 5p, 18p. |
| [a] ctD2 | Plasma (PB) | High MNA | D | *ALK* amplification 11q, 17q. | 1p, 10q. |
| ctD3 | Plasma (PB) | High MNA | D | 1q13.1q32.1, 2p16.1p25.3, *CDK4* amplification, *CCND1* amplification 6p21.3q27, 12p13.3q24.3, 14q11.2q32.12. | X, 11, 9, 10, 4, 5p. |

**Table A1.** *Cont.*

| Sample Name | Sample Type | NB Risk Group and *MYCN* Status | Time Point | SNP Array Data Gain | Loss |
|---|---|---|---|---|---|
| ctD4 | Plasma (PB) | High MNA | D | 17q. | 1p, 3p, 10, 15q. |
| ctD5 | Plasma (PB) | High Non-MNA | D | 11pq, 17q, 18. | 11q. |
| ctD6 | Plasma (PB) | High MNA | D | 2p23.1(*ALK*), 17q. | 1p, 9, 11. |
| ctD7 | Plasma (PB) | High MNA | D | 17q22q25.3. | 1p31.2p36.33. |
| ctD9 | Plasma (PB) | High MNA | D | 16q, 17q, 21. | 1p, 3, 4q, 5pq, 6, 8, 14, 15q, 16q, 17p, CN-LOH: 9, 10, 11, 19, X. |
| ctD10 | Plasma (PB) | High MNA | D | 17p12p11.2, 17q12q22. | 3, 5, 4q, 9, 10, 11, 13q, 21q. |
| [d] ctD11 | Plasma (PB) | High Non-MNA | D | 6p, 7p, 13q, 21 & 12. | 6p, 6q, 8p, 8q, 11, 17p. |
| ctD12 | Plasma (PB) | High Non-MNA | D | 2p, 6pq, 7p, 11p, 12q, 16q, 17q, 22q, 13 & 18. | 9p, 11q. |
| ctD13 | Plasma (PB) | High MNA | D | 17q. | 1p, 3p. |
| ctD14 | Plasma (PB) | Low Non-MNA | D | Whole-chromosome abnormalities only | |
| [e] ctD15 | Plasma (PB) | Low Non-MNA | D | Whole-chromosome abnormalities only | |
| ctD16 | Plasma (PB) | High MNA | D | 1q, 2p, 9q, 11q, 17q, 18p. | 1p, 3p, 11q, X. |
| [f] ctD17 | Plasma (PB) | Int ** Non-MNA | D | 1q, 2p, 5p, 11q, 16q, 17q, 20q. | 3p, 5q, 6p, 6q, 9p (*PTPRD*), 9q, Y. |
| ctD18 | Plasma (PB) | High Non-MNA | D | 1q, 2p (*MYCN*), 12q, 17q, 20q. | 3p, 3q, 11q, 19q, 22q, Xq21.1 (*ATRX*). |
| ctD19 | Plasma (PB) | High MNA | D | 2, 4, 7, 8, 8p11.22p11.21, 12, 15, 17p11.2q25.3, 18, 20, 21, 22, *FGFR1* amplification. | 10 |
| [b] ctD20 | Plasma (PB) | High MNA | D | 3, 11, 14, 20q13.2q13.33, 21, 22. | 1, 2, 8p23.3q21.3, 9, 10p15.3q21.1, 13, 16q11.2q24.3, 18, 17p. |
| [b] ctD21 | Plasma (PB) | High MNA | R | 3, 11, 14, 20q13 2q13.33, 21, 22. | 1, 2, 8p23, 3q21.3, 9, 10p15, 3q21.1, 13, 16q11, 2q24.3, 18, 17p. |
| ctD22 | Plasma (PB) | High Non-MNA | D | 1q21.1q42.2,6, 7, 8p23.3p22,10p15.3q11.21, 13, 17, 18, 20, 21. | 1q42.2q44, 3, 9p24.1 (*PTPRD*), 11, 11q14.1q22.3, 15q13.2q26.3, 19. |
| ctD23 | Plasma (PB) | High Non-MNA | D | 4p16, 3q21.23, 7, 13q11q31.3, 13q32, 1q34, 17, 18. | 1q44, 2q44, 2q21, 3q37.3, 3, 5q15q35.3, 9p24, 3p22.3, 9p21, 3q34.3, 11, 14, 16, 19, 22, X, LOH: 2q21.3q37.3, 5q15q35.3, 11, 16, 22. |

**Table A1.** *Cont.*

| Sample Name | Sample Type | NB Risk Group and *MYCN* Status | Time Point | SNP Array Data | |
| --- | --- | --- | --- | --- | --- |
| | | | | Gain | Loss |
| ctD24 | Plasma (PB) | High Non-MNA | D | 6p, 7pq, 13q, 17pq, 18, 21. | 6q, 7p, 17p. |
| ctD25 | Plasma (PB) | High Non-MNA | D | 1q, 3q, 6p, 3q, 7, 11q, 1q, 12, 16q,17q, 18. | 3p26, 3p12.2, 3p12, 2q29, 4, 6q22, 33q27, 8, 11q13, 3q25, 14, 17p13, 3q21.31, 19p13, 3p13.11. |
| ctD26 | Plasma (PB) | Low Non-MNA | D | 1, 2, 7, 12, 17. | No loss |
| ctD27 | Plasma (PB) | Int Non-MNA | D | 2, 5, 7, 13, 17, 22, X. | 3, 4, 11, 14, 21 LOH: 3, 14. |
| ctD28 | Plasma (PB) | Int ** Non-MNA | D | Tetraploid. | 3, 4, 14, 15, 16. |
| ctD29 | Plasma (PB) | Low Non-MNA | D | No gains. | 2, 3, 4, 11, 12, 14, 15, 16, 19, 21, X CN-LOH: 11. |
| c ctD30 | Plasma (BM) | High Non-MNA | D | * 2p, 6p, 7, 17q, 18. | 3q, 5, 6q, 9p, 10, 11q, 17p, 19. |
| c ctD31 | Plasma (PB) | High Non-MNA | D | * 2p, 6p, 7, 17q, 18. | 3q, 5, 6q, 9p, 10, 11q, 17p, 19. |
| ctD32 | Plasma (PB) | High MNA | R | * 1q, 2p, 11q, 17q,19q, 3, 5, 6, 7, 8, 12, 13, 14, 16, 20, 21. | * 1p, 11q, 19p, 22q. |
| d gD1 | DNA | High | D | - | - |
| e gD2 | DNA | Low | D | - | - |
| f gD3 | DNA | Int ** | D | - | - |
| SH-SY-5Y | DNA | High Non-MNA | R | 1q, 7, 17q. | 14p, 22q. |
| GIMEN | DNA | High Non-MNA | R | 2p. | 1p, 6q, 11q. |
| NB-1691 | DNA | High MNA | R | *ALK, CDK4, MDM2* amp 3q, 5p, 6p, 12, 17. | 3p. |
| SK-N-BE-(2)C | DNA | High MNA | R | 2p. | 1p, 17, 18, X, 11p, 9p, 3p. |
| Control1 | Synthetic plasma | - | - | - | - |
| Control2 | Normal control DNA | - | - | - | - |

*Appendix A.2*

**Table A2.** Gene list for the 42-gene QIASeq custom tNGS panel used in this study.

| Variant Gene | Chromosomal Location | Transcript | Function |
| --- | --- | --- | --- |
| *ALK* | 2p23.1 | NM_004304.4 | Tyrosine kinase |
| *ARID1A* | 1p36.11 | NM_006015.4 | Chromatin remodelling factor |
| *ARID1B* | 6q25.3 | NM_020732.3 | Chromatin remodelling factor |
| *ATM* | 11q22.3 | NM_000051.3 | Serine/threonine kinase |
| *ATRX* | Xq21.1 | NM_000489.3 | Chromatin remodelling factor |
| *BRAF* | 7q34 | NM_004333.4 | Protein kinase |
| *CCND1* | 11q13.3 | NM_053056.2 | Cyclin dependent protein kinase |
| *CDK4* | 12q14.1 | NM_000075.3 | Cyclin dependent protein kinase |

**Table A2.** *Cont.*

| Variant Gene | Chromosomal Location | Transcript | Function |
|---|---|---|---|
| CDK6 | 7q21.2 | NM_001259.6 | Cyclin-dependent protein kinase |
| CDKN2A | 9p21.3 | NM_001195132.1 | Cyclin-dependent protein kinase |
| CDKN2B | 9p21.3 | NM_004936.3 | Cyclin-dependent protein kinase |
| CHEK2 | 22q22.1 | NM_007194.4 | Protein kinase |
| CREBBP | 16p13.3 | NM_004380.3 | Acetyltransferase |
| ERBB2 | 17q12 | NM_004448.2 | Tyrosine kinase |
| FGFR1 | 8p11.23 | NM_001174067.1 | Tyrosine kinase growth factor |
| FGFR4 | 5q35.2 | NM_002011.3 | Growth factor receptor tyrosine kinase |
| HRAS | 11p15.5 | NM_005343.2 | GTPase |
| IDH1 | 2q34 | NM_005896.2 | Catalytic isozyme |
| KMT2C | 7q36.1 | NM_170606.3 | Histone methyltransferase |
| KRAS | 12p12.1 | NM_033360.2 | GTPase |
| LIN28B | 6q16-6q21 | NM_001004317.3 | RNA-binding protein |
| MAP2K1 | 15q22.31 | NM_002755.3 | MAP kinase |
| MAP2K2 | 19p13.3 | NM_030662.3 | Tyrosine kinase |
| MAP3K13 | 3q27.3 | NM_001242314.1 | Serine/threonine kinase |
| MDM2 | 12q15 | NM_002392.4 | TP53 regulator (negative) |
| MDM4 | 1q32.1 | NM_002393.4 | TP53 regulator (negative) |
| MYC | 8q24.21 | NM_002467.4 | Transcription factor |
| MYCN | 2p24.3 | NM_005378.4 | Transcription factor |
| NF1 | 17q11.2 | NM_001042492.2 | Tumour suppressor |
| NRAS | 1p13.2 | NM_002524.4 | GTPase |
| PDE6G | 17q25.3 | NM_002602.3 | Phosphodiesterase |
| PDGFRA | 4q12 | NM_006206.4 | Tyrosine kinase |
| PHOX2B | 4p13 | NM_003924.3 | Transcription factor |
| PIK3CA | 3q26.32 | NM_006218.2 | Lipid kinase |
| PTCH1 | 9q22.32 | NM_000264.3 | Receptor for Hedgehog genes |
| PTEN | 10q23.31 | NM_000314.4 | Phosphatase |
| PTPN11 | 12q24.13 | NM_002834.3 | Protein tyrosine phosphatase |
| PTPRD | 9p23 | NM_002839.3 | Tyrosine phosphatase |
| SMARCA4 | 19p13.2 | NM_003072.5 | Chromatin regulator |
| TENM3 | 4q34.3 | NM_001080477.1 | Neuronal development protein |
| TP53 | 17p13.1 | NM_000546.6 | Tumour suppressor |
| TSC1 | 5q32-q33 | NM_000368.5 | Tumour suppressor |

# References

1. Tolbert, V.P.; Matthay, K.K. Neuroblastoma: Clinical and biological approach to risk stratification and treatment. *Cell Tissue Res.* **2018**, *372*, 195–209. [CrossRef]

2. Matthay, K.K.; Maris, J.M.; Schleiermacher, G.; Nakagawara, A.; Mackall, C.L.; Diller, L.; Weiss, W.A. Neuroblastoma. *Nat. Rev. Dis. Primers* **2016**, *2*, 16078. [CrossRef] [PubMed]

3. Lone, S.N.; Nisar, S.; Masoodi, T.; Singh, M.; Rizwan, A.; Hashem, S.; El-Rifai, W.; Bedognetti, D.; Batra, S.K.; Haris, M.; et al. Liquid biopsy: A step closer to transform diagnosis, prognosis and future of cancer treatments. *Mol. Cancer* **2022**, *21*, 79. [CrossRef] [PubMed]

4. Russano, M.; Napolitano, A.; Ribelli, G.; Iuliani, M.; Simonetti, S.; Citarella, F.; Pantano, F.; Dell'Aquila, E.; Anesi, C.; Silvestris, N.; et al. Liquid biopsy and tumor heterogeneity in metastatic solid tumors: The potentiality of blood samples. *J. Exp. Clin. Cancer Res.* **2020**, *39*, 95, Erratum in *J. Exp. Clin. Cancer Res.* **2020**, *39*, 120. [CrossRef]

5. Diehl, F.; Schmidt, K.; Choti, M.A.; Romans, K.; Goodman, S.; Li, M.; Thornton, K.; Agrawal, N.; Sokoll, L.; Szabo, S.A.; et al. Circulating mutant DNA to assess tumor dynamics. *Nat. Med.* **2008**, *14*, 985–990. [CrossRef]

6. Lodrini, M.; Graef, J.; Thole-Kliesch, T.M.; Astrahantseff, K.; Sprüssel, A.; Grimaldi, M.; Peitz, C.; Linke, R.B.; Hollander, J.F.; Lankes, E.; et al. Targeted Analysis of Cell-free Circulating Tumor DNA is Suitable for Early Relapse and Actionable Target Detection in Patients with Neuroblastoma. *Clin. Cancer Res.* **2022**, *28*, 1809–1820. [CrossRef]

7. Kahana-Edwin, S.; Cain, L.E.; McCowage, G.; Darmanian, A.; Wright, D.; Mullins, A.; Saletta, F.; Karpelowsky, J. Neuroblastoma Molecular Risk-Stratification of DNA Copy Number and ALK Genotyping via Cell-Free Circulating Tumor DNA Profiling. *Cancers* **2021**, *13*, 3365. [CrossRef]

8. Lodrini, M.; Wünschel, J.; Thole-Kliesch, T.M.; Grimaldi, M.; Sprüssel, A.; Linke, R.B.; Hollander, J.F.; Tiburtius, D.; Künkele, A.; Schulte, J.H.; et al. Circulating Cell-Free DNA Assessment in Biofluids from Children with Neuroblastoma Demonstrates Feasibility and Potential for Minimally Invasive Molecular Diagnostics. *Cancers* **2022**, *14*, 2080. [CrossRef]

9. Chan, K.C.; Jiang, P.; Zheng, Y.W.; Liao, G.J.; Sun, H.; Wong, J.; Siu, S.S.; Chan, W.C.; Chan, S.L.; Chan, A.T.; et al. Cancer genome scanning in plasma: Detection of tumor-associated copy number aberrations, single-nucleotide variants, and tumoral heterogeneity by massively parallel sequencing. *Clin. Chem.* **2013**, *59*, 211–224. [CrossRef]

10. Leary, R.J.; Sausen, M.; Kinde, I.; Papadopoulos, N.; Carpten, J.D.; Craig, D.; O'Shaughnessy, J.; Kinzler, K.W.; Parmigiani, G.; Vogelstein, B.; et al. Detection of chromosomal alterations in the circulation of cancer patients with whole-genome sequencing. *Sci. Transl. Med.* **2012**, *4*, 162ra54. [CrossRef] [PubMed]

11. Tate, J.G.; Bamford, S.; Jubb, H.C.; Sondka, Z.; Beare, D.M.; Bindal, N.; Boutselakis, H.; Cole, C.G.; Creatore, C.; Dawson, E.; et al. COSMIC: The Catalogue Of Somatic Mutations In Cancer. *Nucleic Acids Res.* **2019**, *47*, D941–D947. [CrossRef]

12. Ioannidis, N.M.; Rothstein, J.H.; Pejaver, V.; Middha, S.; McDonnell, S.K.; Baheti, S.; Musolf, A.; Li, Q.; Holzinger, E.; Karyadi, D.; et al. REVEL: An Ensemble Method for Predicting the Pathogenicity of Rare Missense Variants. *Am. J. Hum. Genet.* **2016**, *99*, 877–885. [CrossRef]

13. Allinson, L.M.; Potts, A.; Goodman, A.; Bown, N.; Bashton, M.; Thompson, D.; Basta, N.O.; Gabriel, A.S.; McCorkindale, M.; Ng, A.; et al. Loss of ALK hotspot mutations in relapsed neuroblastoma. *Genes Chromosomes Cancer* **2022**, *61*, 747–753. [CrossRef]

14. George, S.L.; Izquierdo, E.; Campbell, J.; Koutroumanidou, E.; Proszek, P.; Jamal, S.; Hughes, D.; Yuan, L.; Marshall, L.V.; Carceller, F.; et al. A tailored molecular profiling programme for children with cancer to identify clinically actionable genetic alterations. *Eur. J. Cancer* **2019**, *121*, 224–235. [CrossRef] [PubMed]

15. George, S.L.; Lynn, C.; Stankunaite, R.; Hughes, D.; Sauer, C.M.; Chalker, J.; Waqar Ahmed, S.; Oostveen, M.; Proszek, P.Z.; Yuan, L.; et al. Stratified Medicine Pediatrics: Cell-Free DNA and Serial Tumor Sequencing Identifies Subtype-Specific Cancer Evolution and Epigenetic States. *Cancer Discov.* **2025**, *15*, 717–732. [CrossRef] [PubMed]

16. Jongmans, M.C.J.; van der Burgt, I.; Hoogerbrugge, P.M.; Noordam, K.; Yntema, H.G.; Nillesen, W.M.; Kuiper, R.P.; Ligtenberg, M.J.; van Kessel, A.G.; van Krieken, J.H.; et al. Cancer risk in patients with Noonan syndrome carrying a PTPN11 mutation. *Eur. J. Hum. Genet.* **2011**, *19*, 870–874. [CrossRef]

17. Mutesa, L.; Pierquin, G.; Janin, N.; Segers, K.; Thomée, C.; Provenzi, M.; Bours, V. Germline PTPN11 missense mutation in a case of Noonan syndrome associated with mediastinal and retroperitoneal neuroblastic tumors. *Cancer Genet. Cytogenet.* **2008**, *182*, 40–42. [CrossRef]

18. Ijiri, R.; Tanaka, Y.; Keisuke, K.; Masuno, M.; Imaizumi, K. A case of Noonan's syndrome with possible associated neuroblastoma. *Pediatr. Radiol.* **2000**, *30*, 432–433. [CrossRef] [PubMed]

19. Merugu, S.; Chen, L.; Gavens, E.; Gabra, H.; Brougham, M.; Makin, G.; Ng, A.; Murphy, D.; Gabriel, A.S.; Robinson, M.L.; et al. Detection of Circulating and Disseminated Neuroblastoma Cells Using the ImageStream Flow Cytometer for Use as Predictive and Pharmacodynamic Biomarkers. *Clin. Cancer Res.* **2020**, *26*, 122–134. [CrossRef]

20. Amoroso, L.; Ognibene, M.; Morini, M.; Conte, M.; Di Cataldo, A.; Tondo, A.; D'Angelo, P.; Castellano, A.; Garaventa, A.; Lasorsa, V.A.; et al. Genomic coamplification of CDK4/MDM2/FRS2 is associated with very poor prognosis and atypical clinical features in neuroblastoma patients. *Genes Chromosomes Cancer* **2020**, *59*, 277–285. [CrossRef]

21. Rihani, A.; Vandesompele, J.; Speleman, F.; Van Maerken, T. Inhibition of CDK4/6 as a novel therapeutic option for neuroblastoma. *Cancer Cell Int.* **2015**, *15*, 76. [CrossRef] [PubMed]

22. Tucker, E.R.; Jiménez, I.; Chen, L.; Bellini, A.; Gorrini, C.; Calton, E.; Gao, Q.; Che, H.; Poon, E.; Jamin, Y.; et al. Combination Therapies Targeting ALK-aberrant Neuroblastoma in Preclinical Models. *Clin. Cancer Res.* **2023**, *29*, 1317–1331. [CrossRef] [PubMed]

23. Bagley, S.J.; Nabavizadeh, S.A.; Mays, J.J.; Till, J.E.; Ware, J.B.; Levy, S.; Sarchiapone, W.; Hussain, J.; Prior, T.; Guiry, S.; et al. Clinical Utility of Plasma Cell-Free DNA in Adult Patients with Newly Diagnosed Glioblastoma: A Pilot Prospective Study. *Clin. Cancer Res.* **2020**, *26*, 397–407. [CrossRef]

24. Fleischhacker, M.; Schmidt, B.; Weickmann, S.; Fersching, D.M.; Leszinski, G.S.; Siegele, B.; Stötzer, O.J.; Nagel, D.; Holdenrieder, S. Methods for isolation of cell-free plasma DNA strongly affect DNA yield. *Clin. Chim. Acta* **2011**, *412*, 2085–2088. [CrossRef]

25. Page, K.; Guttery, D.S.; Zahra, N.; Primrose, L.; Elshaw, S.R.; Pringle, J.H.; Blighe, K.; Marchese, S.D.; Hills, A.; Woodley, L.; et al. Influence of plasma processing on recovery and analysis of circulating nucleic acids. *PLoS ONE* **2013**, *8*, e77963. [CrossRef]

26. Bosse, K.R.; Giudice, A.M.; Lane, M.V.; McIntyre, B.; Schürch, P.M.; Pascual-Pasto, G.; Buongervino, S.N.; Suresh, S.; Fitzsimmons, A.; Hyman, A.; et al. Serial Profiling of Circulating Tumor DNA Identifies Dynamic Evolution of Clinically Actionable Genomic Alterations in High-Risk Neuroblastoma. *Cancer Discov.* **2022**, *12*, 2800–2819. [CrossRef] [PubMed]

27. Chicard, M.; Colmet-Daage, L.; Clement, N.; Danzon, A.; Bohec, M.; Bernard, V.; Baulande, S.; Bellini, A.; Deveau, P.; Pierron, G.; et al. Whole-Exome Sequencing of Cell-Free DNA Reveals Temporo-spatial Heterogeneity and Identifies Treatment-Resistant Clones in Neuroblastoma. *Clin. Cancer Res.* **2018**, *24*, 939–949. [CrossRef]

28. Bobin, C.; Iddir, Y.; Butterworth, C.; Masliah-Planchon, J.; Saint-Charles, A.; Bellini, A.; Bhalshankar, J.; Pierron, G.; Combaret, V.; Attignon, V.; et al. Sequential Analysis of cfDNA Reveals Clonal Evolution in Patients with Neuroblastoma Receiving ALK-Targeted Therapy. *Clin. Cancer Res.* **2024**, *30*, 3316–3328. [CrossRef]

29. Berko, E.R.; Witek, G.M.; Matkar, S.; Petrova, Z.O.; Wu, M.A.; Smith, C.M.; Daniels, A.; Kalna, J.; Kennedy, A.; Gostuski, I.; et al. Circulating tumor DNA reveals mechanisms of lorlatinib resistance in patients with relapsed/refractory ALK-driven neuroblastoma. *Nat. Commun.* **2023**, *14*, 2601. [CrossRef]

30. Mossé, Y.P.; Laudenslager, M.; Longo, L.; Cole, K.A.; Wood, A.; Attiyeh, E.F.; Laquaglia, M.J.; Sennett, R.; Lynch, J.E.; Perri, P.; et al. Identification of ALK as a major familial neuroblastoma predisposition gene. *Nature* **2008**, *455*, 930–935. [CrossRef]

31. Bresler, S.C.; Weiser, D.A.; Huwe, P.J.; Park, J.H.; Krytska, K.; Ryles, H.; Laudenslager, M.; Rappaport, E.F.; Wood, A.C.; McGrady, P.W.; et al. ALK mutations confer differential oncogenic activation and sensitivity to ALK inhibition therapy in neuroblastoma. *Cancer Cell* **2014**, *26*, 682–694. [CrossRef] [PubMed]

32. Ackermann, S.; Cartolano, M.; Hero, B.; Welte, A.; Kahlert, Y.; Roderwieser, A.; Bartenhagen, C.; Walter, E.; Gecht, J.; Kerschke, L.; et al. A mechanistic classification of clinical phenotypes in neuroblastoma. *Science* **2018**, *362*, 1165–1170. [CrossRef]

33. Rahmqvist, I.; Engström, E.; Mellström, E.; Ibrahim, R.R.; Pujol-Calderón, F.; Dahlstrand Rudin, A.; Ordqvist Redfors, A.; Rostamzadeh, N.; Di Rienzo, R.; Franssila, W.; et al. Personalized circulating tumor DNA analysis for sensitive disease monitoring and detection of relapse in neuroblastoma. *Biomark. Res.* **2024**, *12*, 148. [CrossRef]

34. Ek, T.; Ibrahim, R.R.; Vogt, H.; Georgantzi, K.; Träger, C.; Gaarder, J.; Djos, A.; Rahmqvist, I.; Mellström, E.; Pujol-Calderón, F.; et al. Long-Lasting Response to Lorlatinib in Patients with ALK-Driven Relapsed or Refractory Neuroblastoma Monitored with Circulating Tumor DNA Analysis. *Cancer Res. Commun.* **2024**, *4*, 2553–2564. [CrossRef]

35. Chen, L.; Humphreys, A.; Turnbull, L.; Bellini, A.; Schleiermacher, G.; Salwen, H.; Cohn, S.L.; Bown, N.; Tweddle, D.A. Identification of different ALK mutations in a pair of neuroblastoma cell lines established at diagnosis and relapse. *Oncotarget* **2016**, *7*, 87301–87311. [CrossRef] [PubMed]

36. McLaren, W.; Gil, L.; Hunt, S.E.; Riat, H.S.; Ritchie, G.R.; Thormann, A.; Flicek, P.; Cunningham, F. The Ensembl Variant Effect Predictor. *Genome Biol.* **2016**, *17*, 122. [CrossRef]

37. Karczewski, K.J.; Francioli, L.C.; Tiao, G.; Cummings, B.B.; Alföldi, J.; Wang, Q.; Collins, R.L.; Laricchia, K.M.; Ganna, A.; Birnbaum, D.P.; et al. The mutational constraint spectrum quantified from variation in 141,456 humans. *Nature* **2020**, *581*, 434–443, Erratum in *Nature* **2021**, *590*, E53.

38. Ng, P.C.; Henikoff, S. SIFT: Predicting amino acid changes that affect protein function. *Nucleic Acids Res.* **2003**, *31*, 3812–3814. [CrossRef]

39. Adzhubei, I.; Jordan, D.M.; Sunyaev, S.R. Predicting functional effect of human missense mutations using PolyPhen-2. *Curr. Protoc. Hum. Genet.* **2013**, *76*, 7.20. 1–7.20. 41. [CrossRef]

40. Sherry, S.T.; Ward, M.H.; Kholodov, M.; Baker, J.; Phan, L.; Smigielski, E.M.; Sirotkin, K. dbSNP: The NCBI database of genetic variation. *Nucleic Acids Res.* **2001**, *29*, 308–311. [CrossRef] [PubMed]

41. Eijkelenboom, A.; Tops, B.B.J.; van den Berg, A.; van den Brule, A.J.C.; Dinjens, W.N.M.; Dubbink, H.J.; Ter Elst, A.; Geurts-Giele, W.R.R.; Groenen, P.; Groenendijk, F.H.; et al. Recommendations for the clinical interpretation and reporting of copy number gains using gene panel NGS analysis in routine diagnostics. *Virchows Arch.* **2019**, *474*, 673–680. [CrossRef] [PubMed]